Materials Advances

ROYAL SOCIETY OF CHEMISTRY

REVIEW

View Article Online
View Journal | View Issue

Cite this: *Mater. Adv.*, 2022, 3, 8848

Porous ionic liquids: beyond the bounds of free volume in a fluid phase†

Jocasta Avila, Ryan Clark, Agilio A. H. Pádua and Margarida Costa Gomes *

After reviewing the synthesis, characterisation and applications of more than 150 porous suspensions reported so far in the literature, we conclude that type III porous liquids are either suspensions of pristine MOFs in ionic liquids and liquid polymers or of decorated MOFs in molecular solvents. The first are always stable suspensions, keep the ionic liquids structure and properties and are commonly designated as porous ionic liquids. Original calorimetry measurements reveal a drastic change on the heat effect measured when different MOFs are dispersed in the same ionic liquid or when ZIF-8 is dispersed in different ionic liquids pointing towards distinct solid-ionic liquid interactions. By associating these findings with molecular simulations we highlight the molecular reasons that explain the stability of the porous suspensions which depends not only on the solid-ionic liquid affinity but also on the structure of the ionic liquids near the solid particles. The unique properties of porous ionic liquids thus go beyond those of type III porous liquids in general. They are a new family of porous materials with great potential for all applications where solvents capable of dissolving large quantities of gases or small molecules are required.

Received 19th June 2022,
Accepted 25th October 2022

DOI: 10.1039/d2ma00712f

rsc.li/materials-advances

1 Introduction

Porous liquids were first conceptualized in 2007[1] and then prepared and characterised in 2015.[2] When porous liquids are prepared as neat liquid materials with intrinsic porosity (type I porous liquids) they consist of molecules with permanent and stable internal cavities that do not interpenetrate. Type I porous liquids can have very large cavities but a considerable synthesis effort is required and the properties of the final material, including its melting point and viscosity, are difficult to predict beforehand.

When the cage molecule is solid or too viscous to be easily used in most applications, it can be dissolved in an appropriate bulky solvent to produce a fluid with permanent porosity[2] commonly designated as type II porous liquid. An alternative route for fluids with permanent porosity is possible by pushing this approach further and use porous solids, stably disperse them in voluminous liquids not able to enter the solid pores, and form type III porous liquids. This last route opens a myriad of opportunities to easily prepare fluids with permanent porosity. Type I porous liquids still remain attractive as pure substances, often non-volatile as they include no solvents.

Porous liquids share the properties of porous solids but they are not just another family of porous materials.[3] Mechanical fatigue, physical aging or plasticization, common in solid sorbent materials,[4] are absent in porous fluid phases that present numerous additional advantages for continuous processes. Porous liquids can be pumped, have large absorption capacities, their pores are easily wet and their regeneration or reuse is simpler than for solid sorbents.[5] Furthermore, they allow the use of existing infrastructures for separations, reactions or other processes. Porous liquids can easily be prepared for specific tasks requiring the presence of cavities, the most evident applications being in the separation of relatively small molecules such as gases near room conditions,[5,6] or as solvents in reactions involving gases.[7] Being such a vast family of fluids, porous liquids can impact any area that uses liquid solvents making fluids with unique properties available, far beyond the mere increase of permanent free volume.

The preparation of type III porous liquids is generally favoured when compared to type I or type II which require considerable synthesis efforts under harsh conditions, often with low yield. Type III porous liquids have been prepared at milder, environmentally friendly conditions from available, relatively cheap starting materials and can be designed to gather the properties of the liquid and of the dispersed porous scaffolds.[5,8] The design of type III porous liquids thus involve the appropriate choice of the porosity generator materials and of the sterically hindered liquids where they will be dispersed in. Both are crucial to obtain a porous liquid as a stable suspension[8,9] that will not limit scale-up or application when stirring is not involved[10] with a sufficiently low vapour pressure to facilitate recycling. Appropriate constituents of

Laboratoire de Chimie, CNRS and Ecole Normale Supérieure de Lyon, 46 allée dItalie, 69364 Lyon, France. E-mail: margarida.costa-gomes@ens-lyon.fr

† Electronic supplementary information (ESI) available. See DOI: https://doi.org/10.1039/d2ma00712f

the porous liquid suspension should also lead to fluid materials that are thermally and chemically stable with relatively small pores and controlled fluidity.[11] Non-volatility can be achieved, even at relatively high temperatures, when using ionic liquids in the preparation of type III porous liquids.[12]

Herein we will review the synthesis, characterization and applications of type III porous liquids. The permanent porosity in these materials have so far been achieved through the use of metal–organic frameworks (MOFs), metal organic polyhedrals (MOPs), porous carbon or zeolites that have been dispersed in different organic solvents, polymers or ionic liquids. The approaches made by different research groups to engineer type III porous liquids will be reported. So far stable porous suspensions with appropriate viscosity, volatility and selectivity towards the absorption of different solutes have been achieved by choosing suitable components but also by the surface functionalization of the solid, the control of the particle sizes or by mastering the interactions between the solvent and the solid.[9,11]

We will address some of the challenges prevailing in the generalised use of type III porous liquids[9] by reviewing recent results on the thermodynamics of absorption of different gases (chemically or physically) and by reporting original data on the microscopic structure of MOF-based porous ionic liquids and on the energies of interaction of different MOFs with ionic solvents obtained by precise dissolution calorimetry measurements. The traditional methods used for the characterization of porosity in solids might not be straightforward when it comes to the application of these methods to porous liquids,[9] and the same can be said for the physical–chemical characterisation of the suspensions using techniques developed for homogeneous liquid phases. These difficulties will be discussed and some recommendations will be made, namely for type III porous liquids based on ionic liquids (PoILs).

2 Reported type III porous liquids

At least one hundred and fifty different type III porous liquids have been reported so far as listed chronologically in Table 1 which includes details of the liquid solvents, of the porous solids suspended with their concentration, and an indication of the stability of the suspensions. All the listed suspensions are fluids with permanent porosity as proven by an enhanced gas absorption when compared with the pure solvent used in their preparation.

The porous liquids in Table 1 consist of pristine solid porous scaffolds – metal organic frameworks, zeolites, porous organic polymers, porous organic cages, or hollow carbon nanospheres – dispersed in appropriate liquids. All the solids and solvents mentioned with abbreviations are listed in ESI.† Only about one fifth of the described suspensions are stable for more than one day. These correspond either to metal organic frameworks dispersed in ionic liquids and heavy poly(dimethyl)siloxane or to decorated metal organic frameworks dispersed in molecular solvents.[4,13]

The first type III porous liquid was reported in 2014 and aimed at using the unique properties of MOFs as gas adsorbents while avoiding the main difficulties of conventional solid–absorption processes.[14] The solids were made available in a liquid slurry and the authors noted for the first time that the combination of MOFs with liquid solvents allows the introduction of a new dimension on the design of absorbents with task-specific properties. In 2018, three different research groups independently took this concept further by combining MOFs or zeolites with ionic liquids to form porous suspensions. Shan *et al.*[15] chose an ionic liquid based on a voluminous dication where they suspended ZIF-8, ZSM-5 and Silicate-1, while Liu *et al.*[16] and Costa Gomes *et al.*[12] chose commercial ionic liquids based on pyridinium or alkylphosphonium cations that proved to be too voluminous to enter ZIF-8 pores. The authors correctly realised that, given the vast number of microporous framework materials and nearly infinite ionic liquids, the difficulty will be to choose the most appropriate pair to design the porous liquid required for a given application. Molecular simulation was soon pointed out as a valuable tool to understand, at the molecular level, the porous suspensions and to identify appropriate MOF–ionic liquid pairs.[12]

Ionic liquids continued to be used to prepare porous liquids associated with small-pore MOFs such as ZIF-8, ZIF-67 or HKUST-1, to create suspensions stable for several months. Alkylphosphonium based ionic liquids with different anions (halogenates, carboxylates or bis-trifluoromethylsulfonylimides) are commonly used for this purpose.[6–8] Other ionic liquids have been explored too, Wang *et al.*[17] chose the pyridinum-based salt proposed initially by Shan *et al.*[15] and Li *et al.*[18] followed the concept of Shan *et al.*[15] and used an imidazolium-based dicationic ionic liquid. Ionic liquids have also shown potential to stably disperse a covalent organic framework (COF) to form a colloidal COF-based porous liquid, which was reported for the first time by Mow *et al.*[19] The liquid salt 3-(3-(4-formylphenoxy propyl)-1-methyl-1*H*-imidazol-3-ium) was chosen to react at the COF's surface and wasshown to be size-excluded from its pores.

Since 2019 several stable porous suspensions made use of decorated solid particles, zeolites or MOFs, in order to avoid aggregation due to gravity or particle–particle attraction. Li *et al.*[20] dispersed H-form zeolites in alkylphosphonium or quaternary ammonium-based ionic liquids while He *et al.*[4] and Li *et al.*[21] coated MOFs with polydimethylsiloxane (PDMS) or polyethyleneimide (BPEI) before stably dispersing the particles in the same silicone oil or in branched BPEI, respectively.[21] The authors claim that favourable particle–liquid interactions explain the stability of the suspensions. Outer surface functionalisation of MOF particles was the solution adopted by Knebel *et al.*[13] to create stable suspensions of large particles of ZIF-67 in common molecular solvents, allowing for processing crystalline materials in a liquid phase.

Cahir *et al.*[10] explored a large universe of solids and liquids to prepare porous liquids, rarely being able to obtain suspensions stable for more than some days. In their case, suspension stability was mainly controlled hydrodynamically by appropriately choosing liquids with high viscosity. A range of porous solids – MOFs, zeolites and porous organic polymers – were dispersed in silicone oils, natural triglycerides, organic polymers and in ionic liquids

Table 1 Type III porous liquids reported in the literature. Indicated are the concentrations in weight percent of porous scaffold used for the suspension, the liquid solvents and the stability of the suspensions at room conditions

Entry	Porous Solid (%w/w)	Solvent	Stability
Liu *et al.*[14]			
1	ZIF-8 (15%)	Glycol	nr
2	ZIF-8 (15%)	Glycol : methylimidazole (3 : 2)	nr
Shan *et al.*[15]			
3	ZIF-8 (3.2–30%)	[DBU-PEG][NTf_2]	Long
4	ZSM-5 (5.3%)	[DBU-PEG][NTf_2]	Long
5	Silicate-1 (2.1%)	[DBU-PEG][NTf_2]	Long
Liu *et al.*[16]			
6	ZIF-8 (1.4%)	[Bpy][NTf_2]	7 months
Costa Gomes *et al.*[12]			
7	ZIF-8 (2—5%)	[$P_{6,6,6,14}$][NTf_2]	>6 months
Li *et al.*[20]			
8	H-ZSM-5 (40%)	[$P_{4,4,4,2}$][Suc]	>2 h
9	H-ZSM-5 (40%)	[$P_{6,6,6,14}$][Br]	>2 h
10	H-ZSM-5 (40%)	[$N_{1,8,8,8}$][Cl]	>2 h
He *et al.*[4]			
11	UiO-66(185)@xPDMS (33–50%)	PDMS4k	Stable
12	UiO-66-NH_2@xPDMS (50%)	PDMS4k	Stable
13	UiO-66-Br_2@xPDMS (50%)	PDMS4k	Stable
14	UiO-66(484)@xPDMS (33%)	PDMS4k	Stable
15	MIL-101(Cr)@xPDMS (33%)	star-PDMS	nr
16	MIL-101(Cr)@xPDMS (33%)	PDMS9k	nr
Cahir *et al.*[10]			
17	HKUST-1(≈14%)	PDMS(13.6, 30k)	≈1 day
18	HKUST-1(≈12%)	PPMS2.5k	>10 days
19	HKUST-1(≈10%)	Brominated vegetable oil	≈1 day
20	HKUST-1(12.5%)	Olive oil	≈1 day
21	HKUST-1(≈14%)	Castor oil	≈1 day
22	HKUST-1(≈15%)	Sesame oil	≈1 day
23	HKUST-1(≈15%)	Sunflower oil	≈1 day
24	HKUST-1(≈15%)	Safflower oil	≈1 day
25	HKUST-1(≈15%)	Soy bean oil	≈1 day
26	HKUST-1(≈15%)	Corn oil	≈1 day
27	$HKUST\text{-}1_{<50nm}$(≈14%)	PDMS(13.6, 30k)	3 days
28	$HKUST\text{-}1_{400nm}$(≈14%)	PDMS30k	*ca.* 7 days
29	OPOSS-HKUST-1(≈14%)	PDMS(2, 3.5, 13.6, 30k)	3 days
30	ZIF-8(12.5%)	PDMS(2, 3.5, 13.6, 30k)	≈1 day
31	ZIF-8(≈17%)	Paraffin oil	≈1 day
32	ZIF-8(≈10%)	Brominated vegetable oil	≈1 day
33	ZIF-8(12.5%)	Olive oil	≈1 day
34	ZIF-8(≈14%)	Castor oil	≈1 day
35	ZIF-8(≈15%)	Sesame oil	≈1 day
36	ZIF-8(≈15%)	Sunflower oil	≈1 day
37	ZIF-8(≈15%)	Safflower oil	≈1 day
38	ZIF-8(≈15%)	Soy bean oil	≈1 day
39	ZIF-8(≈15%)	Corn oil	≈1 day
40	ZIF-8(≈13%)	Poly(ethyleneglycol)-bis(2-ethylhexanoate)	≈1 day
41	ZIF-8(≈12%)	Poly(ethyleneglycol)-dibenzoate	≈1 day
42	ZIF-8(≈12%)	Poly(ethyleneglycol)acrylate	≈1 day
43	Al(fum)(OH)(12.5%)	PDMS(3.5, 13.6, 30k)	≈1 day
44	$Al(fum)(OH)_{<50nm}$ (12.5%)	PDMS(2, 3.5, 13.6, 30k)	>30 days
45	Al(fum)(OH)(≈17%)	Paraffin oil	≈1 day
46	Al(fum)(OH)(≈10%)	Brominated vegetable oil	≈1 day
47	Al(fum)(OH)(≈15%)	Olive oil	≈1 day
48	Al(fum)(OH)(≈14%)	Castor oil	≈1 day
49	Al(fum)(OH)(≈15%)	Sesame oil	≈1 day
50	Al(fum)(OH)(≈15%)	Sunflower oil	≈1 day
51	Al(fum)(OH)(≈15%)	Safflower oil	≈1 day
52	Al(fum)(OH)(≈15%)	Soy bean oil	≈1 day
53	Al(fum)(OH)(≈15%)	Corn oil	≈1 day
54	SIFSIX-3-Zn(≈14%)	PDMS(13.6 and 30k)	≈1 day
55	SIFSIX-3-Zn(6.3%)	PFPE(Y06)2.4k	≈1 day
56	SIFSIX-3-Zn(≈7%)	PFPE(Krytox 177cSt)	≈1 day
57	SIFSIX-3-Cu(≈14%)	PDMS3.5k	≈1 day
58	SIFSIX-3-Cu(12.5%)	PMPS2.5k	≈1 day
59	SIFSIX-3-Cu(≈15%)	Olive oil	≈1 day
60	SIFSIX-3-Cu(≈14%)	Castor oil	≈1 day
61	SIFSIX-3-Cu(≈15%)	Sesame oil	≈1 day
62	(SIFSIX-3-Cu)(≈15%)	Sunflower oil	≈1 day

Table 1 (*continued*)

Entry	Porous Solid (%w/w)	Solvent	Stability
63	SIFSIX-3-Cu(≈15%)	Safflower oil	≈1 day
64	SIFSIX-3-Cu(≈15%)	Soy bean oil	≈1 day
65	SIFSIX-3-Cu(≈15%)	Corn oil	≈1 day
66	UiO-66(≈17%)	Paraffin oil	≈1 day
67	UiO-66(≈15%)	Sesame oil	≈1 day
68	UiO-66-NH_2(≈15%)	Olive oil	≈1 day
69	ZIF-67(≈14%)	PDMS3.5k	≈1 day
70	ZIF-67(≈15%)	Olive oil	≈1 day
71	MOF-801(≈15%)	Olive oil	≈1 day
72	ZIF-90(≈14%)	PDMS3.5k	≈1 day
73	ZIF-90(≈15%)	Olive oil	≈1 day
74	MIL-53(Al)(≈14%)	PDMS3.5k	≈1 day
75	CAU-10-H(≈15%)	Olive oil	≈1 day
76	CD-MOF-1(≈15%)	Olive oil	≈1 day
77	Zeolite(Sigma)(≈15%)	Olive oil	≈1 day
78	Zeolite(Sigma)(≈14%)	Castor oil	≈1 day
79	Zeolite(Sigma)(≈15%)	Sesame oil	≈1 day
80	Zeolite(Sigma)(≈15%)	Sunflower oil	≈1 day
81	Zeolite(Sigma)(≈15%)	Safflower oil	≈1 day
82	Zeolite(Sigma)(≈15%)	Soy bean oil	≈1 day
83	Zeolite(Sigma)(≈15%)	Corn oil	≈1 day
84	Zeolite 5A(≈15%)	Olive oil	≈1 day
85	Zeolite 5A(12.5%)	Castor oil	≈1 day
86	Zeolite 5A(≈15%)	Sesame oil	≈1 day
87	Zeolite 5A(≈15%)	Sunflower oil	≈1 day
88	Zeolite 5A(≈15%)	Safflower oil	≈1 day
89	Zeolite 5A(≈15%)	Soy bean oil	≈1 day
90	Zeolite 5A(≈15%)	Corn oil	≈1 day
91	Zeolite 13X(≈15%)	Olive oil	≈1 day
92	Zeolite 13X(≈14%)	Castor oil	≈1 day
93	Zeolite 13X(≈15%)	Sesame oil	≈1 day
94	Zeolite 13X(≈15%)	Sunflower oil	≈1 day
95	Zeolite 13X(≈15%)	Safflower oil	≈1 day
96	Zeolite 13X(≈15%)	Soy bean oil	≈1 day
97	Zeolite 13X(≈15%)	Corn oil	≈1 day
98	PAF-1(≈15%)	Olive oil	≈1 day
99	PAF-1(≈14%)	Castor oil	≈1 day
100	PAF-1(≈15%)	Sesame oil	≈1 day
101	PAF-1(≈15%)	Sunflower oil	≈1 day
102	PAF-1(≈15%)	Safflower oil	≈1 day
103	PAF-1(≈15%)	Soy bean oil	≈1 day
104	PAF-1(≈15%)	Corn oil	≈1 day
105	PAF-1(12.5%)	Poly(glycol)dimethylether	≈1 day
Mow *et al.*[19]			
106	COF-300(200)(20%)	BAR^F	>12 months
Knebel *et al.*[13]			
107	ZIF-67-IDip(1–6%)	Mesitylene	Stable
108	ZIF-67-IMes(nr%)	Mesitylene	Stable
109	ZIF-8-Zn-IDip(nr%)	Mesitylene	Stable
110	ZIF-67-IDip(nr%)	Cyclohexane	Stable
111	ZIF-67-IDip(nr%)	Cyclooctane	Stable
112	ZIF-67-IMes(nr%)	Cyclohexane	Stable
113	ZIF-67-IMes(nr%)	Cyclooctane	Stable
Lai *et al.*[22]			
114	HKUST-1(12.5%)	Sesame oil	2 days
115	Zeolite AgA(12.5, 25%)	$[C_4mim][NTf_2]/AgNTf_2$	2 days
116	$Cu(QC)_2$(12.5%)	Sesame oil	14 days
117	ZIF-7(12.5, 25%)	Sesame oil	2 days
Li *et al.*[23]			
118	HCNS(10%)	[M2070][PSS]	>12 h in water
Avila *et al.*[8]			
119	ZIF-8(5 and 10%)	$[P_{6,6,6,14}][NTf_2]$	>2 months
120	ZIF-8(5%)	$[P_{6,6,6,14}][Cl]$	>2 months
121	HKUST-1(5%)	$[P_{6,6,6,14}][NTf_2]$	>2 months
Avila *et al.*[6]			
122	ZIF-8(5%)	$[P_{4,4,4,4}][Lev]$	months
Wang *et al.*[17]			
123	ZIF-8(0.27%)	$[BPy][NTf_2]$	nr
Zhou *et al.*[7]			
124	ZIF-8(5%)	$[P_{4,4,4,8}][Cl]$	months

Table 1 (*continued*)

Entry	Porous Solid (%w/w)	Solvent	Stability
125	ZIF-8(5%)	$[P_{6,6,6,14}][Cl]$	months
126	ZIF-8(5%)	$[P_{6,6,6,14}][Br]$	months
Li *et al.*[18]			
127	ZIF-67(2, 5, 8, 10%)	$[C_6(bmim)_2][NTf_2]_2$	>6 months
128	ZIF-8(2, 5, 8, 10%)	$[C_6(bmim)_2][NTf_2]_2$	>6 months
Kai *et al.*[24]			
129	CC3-R(12.5%)	PDMS0.77k	1 day
130	CC3-S(12.5%)	$[BPy][NTf_2]$	1 day
131	CC3-S(12.2%)	$[P_{6,6,6,14}][NTf_2]$	1 day
132	CC3-S(5.8%)	$[BEMA][NTf_2]$	1 day
133	CC3-R/S_{600nm}(12.5 and 20%)	PDMS0.77k	1 day
134	CC3-R/S_{1200nm}(12.5%)	PDMS0.77k	1 day
135	CC3-R/S_{1200nm}(12.5%)	PMPS2.5k	1 day
136	CC3-R/S_{1200nm}(12.5%)	Olive oil	1 day
137	CC3-R/S_{1200nm}(12.5%)	Sunflower oil	1 day
138	CC3-R/S_{1200nm}(12.5%)	Paraffin oil	1 day
139	CC3-R/S_{1200nm}(5%)	PCTFE	1 day
140	CC3-R/S_{1200nm}(5%)	PFPE(Y06)2.4k	1 day
141	CC3-R/S_{1200nm}(12.5%)	15-crown-5	1 day
142	CC3-R/S_{1200nm}(12.5%)	$[Bmim][NTf_2]$	1 day
143	CC3-R/S_{720nm}(5 and 12.5%)	$[BPy][NTf_2]$	1 day
144	CC3-R/S_{630nm}(12.5 and 20%)	$[BPy][NTf_2]$	1 day
145	CC3-R/S_{630nm}(5%)	$[TBPy][NTf_2]$	1 day
146	CC3-R/S_{630nm}(5%)	$[BBIm][NTf_2]$	1 day
147	CC3-R/S_{940nm}(5%)	PDMS0.77k	1 day
148	CC3-R/CC15-$S_{17000nm}$(12.5%)	PDMS0.77k	1 day
149	CC3-R/CC19-$S_{17000nm}$ (12.5%)	PDMS0.77k	1 day
Li *et al.*[21]			
150	ZIF-8-*g*-BPEI(153)(10, 20, and 30%)	Branched BPEI	>6 months
151	ZIF-8-*g*-BPEI(530)(10, 20, and 30%)	Branched BPEI	>6 months
Chen *et al.*[25]			
152	MCM-22(40%)	$[N_{8,8,8,1}][Cl]$	>24 months
Yang *et al.*[26]			
153	HPMo@ZIF-8(100–150)(3.3%)	$[Emim][NTf_2]$	stable
This work (Fig. S1, ESI)			
154	ZIF-8(5%)	$[P_{6,6,6,14}][NTf_2]$	22 months

In the table, 'nr' stands for 'not reported'; PDMSxk for poly(dimethyl)siloxane xk = M_w/1000 kg mol^{-1}; xPDMS for cross-linked poly(monomethacryloxypropyl)-terminated poly(dimethyl)siloxane; PPMS for poly(phenylmethyl)siloxane; PMPS for Poly(methylphenyl)siloxane; PCTFE for Poly(chlorotrifluoroethylene); PFPE for perfluoropolyether and BPEI for polyethyleneimine.

enriched with silver salts.[22] Interestingly enough, some of the combinations tried in this empirical screening are biocompatible, such as those based in CD-MOFS and olive oil, opening the way to the possibility of their use in biomedical applications.

More recently, Li *et al.*[23] and Kai *et al.*[24] formed porous suspensions using hollow carbon nanospheres and porous organic cages, respectively. Li *et al.*[23] used polymerised ionic liquids while Kai *et al.*[24] tried a variety of molecular liquids, ionic liquids and silicone oils, both research groups obtaining suspension with a very low stability.

Ionic liquids and MOFs appear as the most promising pair to prepare porous liquids, the resulting stable suspensions joining the unique properties of both materials. Ionic liquids present a wide liquidus range, are non-volatile, thermally and chemically stable and their physical and chemical properties can be tuned by the combination of different cations and anions or even by mixing different salts. MOFs also present a high chemical and thermal stability and can be prepared to have different structures and porosities by choosing appropriate metal–ligand combinations. Both materials can then be designed with the desired properties and be associated to form appropriate porous liquids.[8] Several authors have observed that the MOF structure remains intact in the porous liquid and its crystalline structure can easily be identified using X-ray diffraction.[8,12,15,16,20] It is also noteworthy that the characteristic mesoscopic structure of the ionic liquid, typical of the segregation between charged and nonpolar domains, is clearly detected in the porous suspension using small angle X-ray scattering,[8] thus confirming that the porous liquid remains structurally an ionic liquid. So far, MOFs have been selected with pores that are sufficiently small to prevent the solvent from entering the material but are sufficiently large to allow gas adsorption and including the appropriate metal–ligand to enhance solid surface–solvent interactions or selective gas absorption/gas separation. It is pertinent to note that with ionic liquids in particular, the volume of the ion pairs, and not necessarily of the individual atoms, must be large enough to not enter the small pores in the solid.

Branched phosphonium and branched ammonium-based ionic liquids can also stabilize zeolites to form porous suspensions. Zeolites are crystalline aluminosilicates (or silicates) with regular arrangements of micropores, high surface areas, and exchangeable cations. They have attracted immense attention in the field of

gas storage, separations and catalysis due to their highly microporous crystalline structure. The preparation of porous liquids containing zeolites require their combination with large hindered solvents that allow a strong liquid–particle interactions because van der Waals forces in zeolites induce particle aggregation and sedimentation. Surface engineering of zeolites was shown to destroy their microporous structure, the primary advantage and value of the material.[20]

2.1 Preparation of type III porous liquids

Table 2 summarizes the origin and pre-treatment of the solvents and solids used for the preparation of the porous liquids listed in Table 1. Details on the techniques used for the preparation of the suspensions and of the techniques used to probe permanent porosity are also included in Table 2. Fig. 1 shows schematically the route to produce type III porous liquids. The suspensions are prepared in general by dispersing the solid scaffold, in the form of particles of known, uniform size, in the liquid solvent (molecular or ionic liquid) by means of appropriate stirring, sonication or mixing. Some authors report that solid MOFs or zeolites can be directly stabilized in ionic liquids – for example ZIF-8, ZSM-5 or Silicate-1 in [DBU-PEG][NTf_2], ZIF-8 in [Bpy][NTf_2], H-SZM-5 in [$P_{4,4,4,2}$][Suc], [$P_{6,6,6,14}$][Br] and [$N_{8,8,8,1}$][Cl]. Others claim that prior dispersion of the solid in methanol,[15,16] in chloroform,[20] or wetting the solid with methanol prior to stirring (as ZIF-8 in [Bpy][NTf_2]) is necessary in order to control the size of the particle aggregates in the suspensions by promoting their solvation. The auxiliary solvents are easily removed by heating or under primary vacuum. Apart from the works of Liu *et al.*, Costa Gomes *et al.*, Avila *et al.*, and Zhou *et al.*[7,8,12,14] all the other porous solid materials used to produce type III porous liquids were purposely synthesized by the authors.

Costa Gomes *et al.*[12] were the first to prepare type III porous liquids from *off-the-shelf*, easily available, MOFs and ionic liquids. Care was taken to homogenize the size of the dispersed solid particles by means of filtration with a 11 μm sieve, and removing water and other gases from both the ionic liquid and the suspension prior to its use. In this case, porous liquids were obtained by simply stirring ZIF-8 in [$P_{6,6,6,14}$][NTf2] for about 5 minutes under ambient conditions. Following the same simple methodology, Avila *et al.*,[6] Zhou *et al.*,[7] Avila *et al.*[8] reproduced the ZIF-8 in [$P_{6,6,6,14}$][NTf_2] porous liquid and replaced the voluminous bis(trifluoromethylsulfonylamide) anion with smaller halide anions – [$P_{6,6,6,14}$][Cl], [$P_{6,6,6,14}$][Br] – and also used branched (asymmetric or symmetric) phosphonium cations combined with halides and carboxylate anions – [$P_{4,4,4,8}$][Cl], [$P_{4,4,4,4}$][Lev] and [$P_{6,6,6,14}$][NTf_2] + [$P_{4,4,4,4}$][OAc] mixtures – which were all able to directly stabilize ZIF-8 or HKUST-1.

MOFs have also been dispersed in liquids other than ionic liquids to form porous suspensions but in those cases decoration of the solid particles was necessary prior to the preparation of the suspensions. This has been done with polymers,[4] or with appropriate ligands[13] allowing for their dispersion in different molecular liquids or liquid polymers.

The porosity in type III porous liquids have been mainly probed by gas absorption–adsorption. In same cases this has

Table 2 Solvent, solid and suspension preparation and permanent porosity probe

Entry	Solvent	Solid	Suspension	Porosity probe
1–2	Commercial	Commercial	Mixing, room T	CO_2, CH_4, N_2 and H_2 abs.
3–5	Synthesized, mixed with CH_3OH	Synthesized, suspended in CH_3OH, dried at 353 K, degas at 313 K	2 h stir, sonication	CO_2 abs.; PALS
6	Commercial	Synthesized, wet with CH_3OH	Stir at 373 K, vacuum at 373 K	I_2 adsorption; PALS
7	Commercial, dry/degas	Commercial, <11 μm mash	2–5 min stir (430–540 rpm), 24 h degas	CO_2, CH_4, and N_2; MD
8	Synthesized, 24 h dried under P_2O_5 at 333 K	Synthesized, suspended in $CHCl_3$	1 h stir, 72 h dry degas at 353 K	CO_2 abs. PALS, MD
9–10	Commercial	Synthesized, suspended in $CHCl_3$	1 h stir, 72 h dry/degas(353 K)	CO_2 abs. PALS, MD
11–16	Commercial	Synthesized, activated at 393 K	CH_2Cl_2, ultrasonication, dry/degas at 393 K	CO_2, H_2O abs.
17–76 98–105	Commercial	Synthesized, Activated	1–2 h stir	CO_2 abs.
77–97	Commercial	Commercial, activated	1–2 h stir	CO_2 abs.
106	Synthesized,	Synthesized, suspended in C_2H_3N	5 min ultrasonication, dry/degas at 363 K	^{19}F NMR, CO_2, CH_4 abs.
107–113	Commercial, dried 3 Å sieve	Synthesized, kept in glove box	12 h stir at room T	CO_2, CH_4, C_3H_6 and C_3H_8 abs.
114–117	Commercial	Synthesized, activated	2 h stir at 600 rpm	C_2H_6, C_2H_4 abs.
118	Synthesized, mixed with water	Synthesized, dispersed in water	30 min stir, dry under vacuum at 323 K	CO_2 abs.
119–121	Commercial, 72 h dry/degas	Commercial, sieve(11 μm mash)	5 min stir(430–540 rpm), 24 h degas	CO_2, CH_4 abs.
122	Synthesized, 72 h dry/degas	Commercial, sieve(11 μm mash)	5 min stir (430–540 rpm), 24 h degas	CO_2 abs.
123	Synthesized	Synthesized	Ultrasonication 2 h at room T, vacuum at 353 K overnight	$C_3H_4F_4O$ extraction
124–126 154	Commercial, 72 h dry/degas	Commercial, Sieve(11 μm mash)	5 min stir (430–540 rpm), 24 h degas	CO_2 abs.
127–128	Synthesized	Synthesized, dispersed in CH_3OH	24 h stir dry overnight at 333 K	CO_2, N_2, C_7H_8 abs.
198–149	Commercial	Synthesized	Mixing + sonication	CO_2, CH_4 abs.
150–151	Commercial	Synthesized, dispersed in CH_3OH	24 h stir at 600 rpm, dry overnight at 333 K	CO_2, N_2 abs.
152	Commercial	Synthesized, dispersed in $CHCl_3$	1 h stir, 72 h dry/degas at 353 K	PALS and MD.
153	Commercial	Synthesized,	2 h stir/ultrasonication at RT,	SO_2, N_2 abs.

DMF = dimethylformamide, $CHCl_3$ = chloroform, CH_2Cl_2 = dichloromethane, C_2H_3N = acetonitrile, $C_3H_4F_4O$ = 2,2,3,3-tetrafluoro-1-propanol, abs. = gas absorption, PALS = positron annihilation lifetime spectroscopy, MD = molecular dynamics.

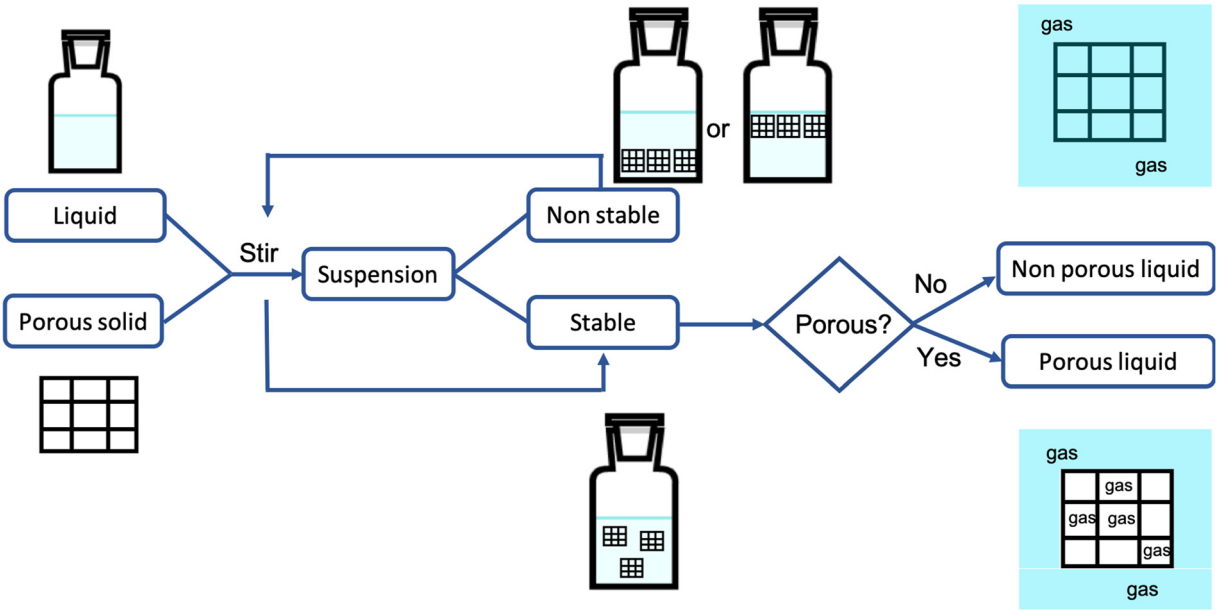

Fig. 1 Schematic route to produce Type III porous liquids: the porous scaffold is properly dispersed in the liquid *via* stirring or ultrasonication, the permanent porosity of the visually stable suspensions (either with or without permanent stirring) are probed mainly by gas absorption. A porous suspension shows an improvement in the gas absorption due to the free volume created in the liquid phase while in a non porous suspension, the liquid is occupying the porous and only the liquid capacity of absorbing the gas is observed. Positron annihililation lifetime spectroscopy (PALS) and molecular dynamics simulation (MD) are also used to probe and predict permanent porosity in porous liquids.

been supported by positron annihilation lifetime spectroscopy (PALS) studies[15,16,20] or by molecular simulation.[12,20]

2.2 Stability of the porous suspensions

The ability of a liquid to house solid particles in suspension to form a type III porous liquid depends on the size, structure and geometry of the pores in the solid, and on the ability of the particles in suspension to aggregate by random movement.

When Mg-MOF-74, a solid in which the pore structure is based on single-type hexagonal channels of about 11 Å, is dispersed in $[P_{6,6,6,14}][NTf_2]$, a voluminous ionic liquid, it does not form a porous liquid. It has been shown both by gas absorption measurements and by molecular simulation that the liquid enters the free pores of the MOF that deposits, filled with the IL, after a few days.[12] If the solids have appropriate pore structure and size and are dispersed in liquids with a sufficiently high molar volume, a porous suspension is normally formed but, as listed in Table 1, it is seldom stable. The stability of the suspensions can be improved either by using viscous solvents thus slowing hydrodynamic processes or by the presence of voluminous solvent molecules, which surround the solid surfaces and hinder particle aggregation especially when solid–solvent interactions are favourable.[8]

The interactions between the porous solids and the solvents can be determined using calorimetric methods by measuring the heat flow involved in the dispersion of the solid in the liquid. We report herein the first such measurements for porous ionic liquids performed in an isothermal dissolution microcalorimeter described in ESI.† The results are summarized in Fig. 2 which shows the heat flow per mass of dispersed solid for ZIF-8 in $[P_{6,6,6,14}][NTf_2]$ and in $[P_{6,6,6,14}][Cl]$ and for HKUST-1 in $[P_{6,6,6,14}][NTf_2]$. We first observe that the kinetics of the wetting process is very different for the three suspensions, the calorimetric signals recovering a stable baseline after 70, 170 and 25 minutes for ZIF-8 in $[P_{6,6,6,14}][NTf_2]$, ZIF-8 in $[P_{6,6,6,14}][Cl]$ and HKUST-1 in $[P_{6,6,6,14}][NTf_2]$, respectively. This is an interesting observation as the two porous solids, ZIF-8 and HKUST-1, are being dispersed into the same ionic liquid at very different rates, meaning that the viscosity is not the determining factor. In this case, it is the wetting of the surface of the MOF which is the determining factor for the kinetics of dissolution. When comparing ZIF-8 in $[P_{6,6,6,14}][NTf_2]$ and $[P_{6,6,6,14}][Cl]$, the kinetics are very different and directly correlated with the different viscosities of the two liquids, the latter being five times more viscous than the former at 323 K.[27]

From Fig. 2 we also conclude that the interactions between the porous solids and the ionic liquids are very different. Indeed, wetting ZIF-8 with both ionic liquids is an exothermic process while the dispersion of HKUST-1 in $[P_{6,6,6,14}][NTf_2]$ is endothermic. Furthermore, the magnitude of the heats involved is quite different, with a significantly higher heat effect for ZIF-8 in $[P_{6,6,6,14}][Cl]$ than for the two other porous dispersions. This last observation means that the interactions between ZIF-8 and $[P_{6,6,6,14}][Cl]$ are more favourable than between ZIF-8 and $[P_{6,6,6,14}][NTf_2]$. This is probably due to a higher affinity of chloride, an anion with localized charge, by the positively charged imidazole surface of ZIF-8 when compared to the voluminous and charge delocalized NTf_2^- anion.

Even though no structural differences were found in the MOF and in the ionic liquid constituting the suspension and

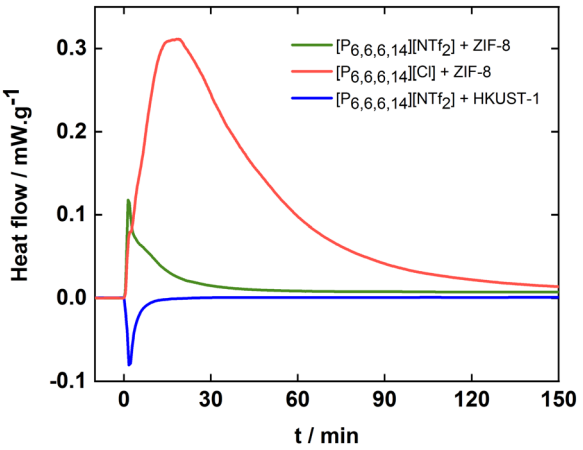

Fig. 2 Average heat change caused by the addition of ZIF-8 in (green) $[P_{6,6,6,14}][NTf_2]$ and (red) $[P_{6,6,6,14}][Cl]$ and of (blue) HKUST-1 in $[P_{6,6,6,14}][NTf_2]$.

besides the ionic liquids viscosity, these calorimetric results clearly show that stable suspensions can be achieved through different mechanisms. For example, by promoting favourable interactions between the porous solid and the liquid or by favouring some other mechanisms, most certainly related to the structural organisation of the liquid near the solid surface. We can then speculate that the stabilization of ZIF-8 in $[P_{6,6,6,14}][NTf_2]$ and $[P_{6,6,6,14}][Cl]$ is governed by favorable molecular interactions (negative enthalpy) while that of HKUST-1 in $[P_{6,6,6,14}][NTf_2]$ depends mainly on structural effects.

This explanation of the stability of the suspensions is confirmed by the molecular simulation snapshots represented in Fig. 3. The top image refers to a simulation box containing a HKUST-1 slab in $[P_{6,6,6,14}][NTf_2]$.[12] It can be seen that the long C_{14} alkyl chains of the phosphonium cation do not fold to accommodate into the surface-accessible cavities of HKUST-1 but instead enter the pores and have their terminal CH_2 and CH_3 groups freely accessing the larger cavities in HKUST-1, a copper benzene-1,3,5-carboxylate salt with 9 Å main channels and tetrahedral-shaped 5 Å side pockets, accessible through a 3 Å triangular window. In the bottom images of Fig. 3 are represented: (i) a slab of ZIF-8 in $[P_{6,6,6,14}][NTf_2]$ (left hand-side) and (ii) the same system but with the solid slab being deleted for clarity (right hand-side). It can be observed that the cation alkyl chains fold and accommodate into the superficial pores of the ZIF-8, a 2-methylimidazle zinc salt with pore apertures of 3.4 Å and pore inner diameter of 11.6 Å. The anchoring of the cations (and corresponding counterions) at the surface of the MOF is likely one of the keys for preventing particle aggregation during long periods of time. ZIF-8 in $[P_{6,6,6,14}][NTf_2]$ suspensions are stable for 22 months (see Fig. S1, ESI†), independently of the MOF concentration (5 or 10%w/w), regular size particle aggregates being stabilized by the ionic liquid. The structure of the solid is maintained after gas absorption and desorption and the typical mesoscopic structure of the ionic liquid is also observed in the suspensions.[8,12]

The high stability of the suspension of H-ZSM-5 in $[P_{6,6,6,14}][Br]$ (entries 8 to 10 in Table 1) observed by Li *et al.*[20] was attributed

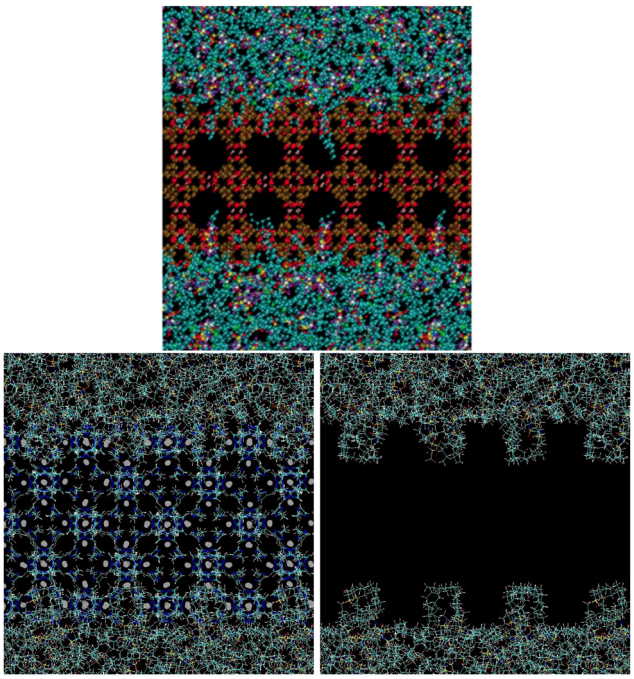

Fig. 3 (Top) Snapshot of a simulation box consisting of $[P_{6,6,6,14}][NTf_2]$ and a slab of HKUST-1.[12] The longer C_{14} alkyl chains of the phosphonium cation enter linearly through the narrow cavities on the MOF surface and the terminal CH_2 and CH_3 are seen freely accessing the larger cavities of HKUST-1. (Bottom) Snapshots of a simulation box consisting of $[P_{6,6,6,14}][NTf_2]$ and a slab of ZIF-8. On the right hand-side image the solid is omitted for the sake of clarity. Grey dots represent Zn atoms, blue the N atoms from the anion and dark yellow the P atoms from the cation.

to the hydrogen bonding between the alkyl chains of the phosphonium cation in the IL and the Brønsted sites in the zeolite nanoparticles and also to the possibility that some alkyl chains enter the zeolite narrow channels and be stabilized by the entropy increase when the free ends are in the larger cavities. A charge transfer to the H-ZSM-5 particles can balance van der Waals forces thus preventing aggregation which is observed by the authors when $[P_{6,6,6,14}][Br]$ and H-ZSM-5 are dispersed in chloroform. The authors observed that the solid crystal structure is always preserved in the suspension.

Shan *et al.*[15] were the first to use ionic liquids and MOFs to produce type III porous liquids, and obtained stable suspensions of ZIF-8, ZSM-5 and Silicate-1 in $[DBU\text{-}PEG][NTf_2]$ for long periods of time. The high stability of the suspension of ZIF-8 in $[DBU\text{-}PEG][NTf_2]$ has been explained by the stable chemical bonding at the solute-solvent interface between the electron-rich nitrogen of the cation and the exposed Zn^{2+} at the solid surface. The authors found, using scanning electron microscopy, that the shape and size of ZIF-8 nanoparticles remain in the ionic liquid. ZIF-8 in $[Bpy][NTf_2]$ suspensions are also stable for large periods (at least 7 months as reported by Liu *et al.*[16]) as verified by the Tyndall effect. Such stability was attributed to the surface groups of ZIF-8 nnoparticles interacting with the ions, preventing particle segregation and leading to colloidal stability.[16] Again the structure of the ZIF-8 particles is preserved after being recovered from the stable colloidal suspensions even seven months after their preparation.

Solid nanosized framework materials do not form stable suspensions in non-ionic liquids. Cahir *et al.*[10] screened several combinations of silicone oils, triglyceride oils and polyethylene glycols with microporous solids such as MOFs, zeolites or porous organic polymers. They concluded that when using sufficiently bulky oil molecules, the stability of the suspensions can be considerably improved from 1 to several days by tuning physical parameters such as solid surface–liquid interaction. This was achieved through important synthesis efforts to prevent particle aggregation by: (i) reducing the solid particle size as in HKUST-1 or Al(fum)OH from 400 Å to <50 Å when dispersed in PDMS; (ii) grafting the solid surfaces with OPOSS (silsesquioxane groups) in HKUST-1 then suspended in PDMS; (iii) modifying a functional group of the solvent as in suspensions of HKUST-1 in polydimethylsiloxane or polyphenyl-methylsiloxane; (iv) increasing the solvent viscosity as in HKUST-1 dispersed in PDMS(20 to 1000 cst); and (v) increasing the density of the solvent using an halogenated oil – Fomblin Y (1.57 g) – where SIFSIX-3-Zn was suspended. Costa Gomes *et al.*[12] also reported that ZIF-8 cannot be stabilized in PEO500, a poly(ethylene glycol) dimethyl ether with M_w = 500 g mol^{-1}, in which the MOF precipitates after a few minutes.

Liu *et al.*[14] who were the pioneers in preparing type III porous liquids, reported that glycol/ZIF-8, glycol-mIm/ZIF-8 and triethylene glycol/ZIF-8 slurries – the solvent molecules forming a film surrounding the solid particles – do not show any loss of mass after 33 gas absorption–desorption cycles and that the structure of the solid remains intact. The slurries were recovered and the permanent porosity preserved at each cycle. Other liquids such as ethanol, cyclohexane, *n*-hexane, methylbenzene and tetrachloromethane do not form stable suspensions of ZIF-8 and they are small enough to enter the pores of the framework material.

He *et al.*[4] produced stable and homogeneous porous suspensions by suspending a polymer coated MOF with different particle size and pore functionality. The functionalized porous material was obtained by growing a layer of PDMS-tethered methacrylate on the MOF surface through a non-covalent based surface-initiated atom transfer radical polymerization (SI-ATRP) in PDMS. The surface modified MOF presents a core–shell structure with preserved crystallinity, the polymer decoration on the MOF surface minimizing particle aggregation. The suspension of UiO-66(185)@xPDMS(50%) in PDMS4k suspension remains stable, with no apparent phase separation, even after centrifuging at 5000 rpm during 5 min.

The MOF surface modification strategy was also employed by Knebel *et al.*[13] to disperse ZIF-67 and ZIF-8 in mesitylene. NHC-based surface modifiers such as the carbenes IMes and IDip were used due to their high reactivity towards unsaturated metal sites and their chemical similarity with the imidazole linker of ZIFs. The surface functionalization did not affect the integrity of the ZIF structure. Modified ZIF-67 formed a stable colloidal dispersion in mesitylene, which was not the case of modified ZIF-8. Contrary to ZIF-8, ZIF-67 has abundant unsaturated metal ions (Co(II)) on its outer surface, which facilitate their coordination with the carbenes. The addition of Zn(II) atoms to the ZIF-8 surface promoted the successful surface modification and the formation of stable colloidal suspensions in mesitylene. Stable dispersions of modified ZIF-67 were also obtained in cyclohexane and cyclooctane.

2.3 Applications of type III porous liquids

Gas absorption measurements have proven as the most straightforward method to probe porosity in stable suspensions of porous solids in liquids. It has been irrevocably shown that when a type III porous liquid is prepared, gas absorption is improved, when compared to the pure solvent, proportionally to the quantity of porous material dispersed. Carbon dioxide is the most used probe gas as listed in Table 3 for a large majority of the the porous liquids reviewed herein (the entry numbers are the same as those in Table 1). Also indicated are the gas capacities of the porous suspensions at the temperatures and pressures studied, the methods used by the different authors and the enthalpy of gas absorption, when available.

In order to better understand the values in Table 3, we can consider aqueous solutions of 2-(dimethylamino)ethanol, DMEA and *N*-ethyldiethanolamine, EDEA, as benchmarks for carbon dioxide absorption with capacities of up to $\approx$3.0 and $\approx$1.8 mmol at 1 bar and 313 K, respectively.[28] Several porous liquids in Table 2 absorb similar quantities of carbon dioxide, remarkable cases being reported by Liu *et al.*[14] for suspensions of ZIF-8 in glycol; Shan *et al.*[15] for ZIF-8 in [DBU-PEG][NTf$_2$]; He *et al.*[4] for suspensions of decorated UiO-66 in PDMS4K; Li *et al.*[23] for carbon nanospheres in [M$_{2070}$][PSS], a polymerized IL; Avila *et al.*[6] for suspensions of ZIF-8 in [P$_{4,4,4,4}$][Lev]; Li *et al.*[18] for suspensions of ZIF-67 in a dicationic ionis liquid ([C$_6$(bmim)$_2$][NTf$_2$]) and Li *et al.*[21] for suspensions of decorated ZIF-8 in branched polyethyleneimine. All these porous liquids absorb more than 1 mmol g^{-1} of CO_2, in general following physisorption mechanisms. This means that, contrary to the aqueous solutions of amines that undergo a chemical reaction with CO_2, gas absorption is easily reversible with a lower energy cost. The enthalpy of CO_2 absorption is less negative, about -9.3 to -14.4 kJ mol^{-1} in porous ionic liquids[8] and 29 kJ mol^{-1} in the suspension of ZIF-8 in glycol-mIm,[14] compared to about 100 kJ mol^{-1} in aqueous alkanolamines.[29]

Porous ionic liquids based on 30%w/w of ZIF-8 suspended in [DBU-PEG][NTf$_2$] show a CO_2 absorption 4.7 times higher than the pure ionic liquid at 10 bar and 298 K.[15] Replacing [DBU-PEG][NTf$_2$] with [P$_{6,6,6,14}$][NTf2] creates a porous ionic liquid suspension capable of absorbing 63% more CO_2 at 5 bar and 303 K and more than 100% CH_4 and N_2 with only 5%w/w of ZIF-8. Methane and nitrogen are scarcely soluble in the pure ionic liquid, thus, the remarkable enhancement is attributed to the free volume of porous solid.[12] Li *et al.*[20] have made similar observations in porous ionic liquids based on the zeolite H-ZSM-5 dispersed in another phosphonium-based IL, [P$_{6,6,6,14}$][Br]. Liu *et al.*,[16] on the other hand, studied 1.4%w/w ZIF-8 suspensions in [Bpy][NTf$_2$] and found that neither CO_2 nor CH_4 could be used to probe the permanent porosity in the suspension because of the relatively low content of ZIF-8 and of the high solubility of the gases in the IL (for that reason no value for CO_2 absorption is listed in Table 3). I_2, however, was

Table 3 CO_2 absorption in the Type III porous liquids. β represents the absorption of the solid in the porous liquid relative to that of the pure solid. The enthalpy of the gas absortion is also indicated in the table

Entry	Method	T/K	p/bar	b_{gas}/mmol g^{-1}	β/%	ΔH_{abs}/kJ mol^{-1}
1	Sapphire cell	293	19.4	≈1.62[a]	73	—
2	Sapphire cell	303	6	≈0.45[a]	74	−29
3	Gravimetric (IGA)	298	10	0.49, 0.81, 1.17, 1.56	90, 85, 76, 74	—
4	Gravimetric (IGA)	298	10	0.46	100	—
5	Gravimetric (IGA)	298	10	0.38	100	—
7	Gravimetric (IGA)	303	5	0.37, 0.47	90, 95	—
8	Gravimetric (IGA)	298	10	≈0.9		—
9	Gravimetric (IGA)	298	10	≈0.5	28	—
10	Gravimetric (IGA)	298	10	≈0.4		—
11	BET (BelsorpII)	273	1	≈1.24[b]	83	—
12	BET (BelsorpII)	273	1	≈1.18[b]	79	—
13	BET (BelsorpII)	273	1	≈0.50[b]	85	—
15	BET (BelsorpII)	273	1	≈0.36[b]	47	—
16	BET (BelsorpII)	273	1	≈0.40[b]	47	—
17	Isochoric	298	0.85	0.56, 0.52	100, 99	—
18	Isochoric	298	0.85	0.56	100	—
19	Isochoric	298	0.85	0.56	99.5	—
20	Isochoric	298	0.85	0.57	99.7	—
21	Isochoric	298	0.85	0.53	98.7	—
22	Isochoric	298	0.85	0.54	99.2	—
23	Isochoric	298	0.85	0.57	99.7	—
24	Isochoric	298	0.85	0.58	100	—
25	Isochoric	298	0.85	0.54	99.2	—
26	Isochoric	298	0.85	0.58	100	—
30	Isochoric	298	0.85	0.2, 0.22, 0.2, 0.18	99.6, 100, 98.8, 95.2	—
31	Isochoric	298	0.85	0.19	100	—
32	Isochoric	298	0.85	0.17	96.4	—
33	Isochoric	298	0.85	0.21	100	—
34	Isochoric	298	0.85	0.19	100	—
35	Isochoric	298	0.85	0.20	100	—
36	Isochoric	298	0.85	0.18	100	—
37	Isochoric	298	0.85	0.18	100	—
38	Isochoric	298	0.85	0.18	100	—
39	Isochoric	298	0.85	0.20	100	—
40	Isochoric	298	0.85	0.26	100	—
41	Isochoric	298	0.85	0.15	98.8	—
42	Isochoric	298	0.85	0.17	96.4	—
43	Isochoric	298	0.85	0.36, 0.38, 0.38	99.5, 100, 100	—
45	Isochoric	298	0.85	0.31	97.7	—
46	Isochoric	298	0.85	0.37	100	—
47	Isochoric	298	0.85	0.35	100	—
48	Isochoric	298	0.85	0.32	98.6	—
49	Isochoric	298	0.85	0.36	100	—
50	Isochoric	298	0.85	0.35	99.5	—
51	Isochoric	298	0.85	0.36	100	—
52	Isochoric	298	0.85	0.34	100	—
53	Isochoric	298	0.85	0.35	100	—
54	Isochoric	298	0.85	0.41, 0.38	100, 99	—
55	Isochoric	298	0.85	0.19	97.4	—
56	Isochoric	298	0.85	nr	nr	—
57	Isochoric	298	0.85	0.37	98.3	—
58	Isochoric	298	0.85	0.40	100	—
59	Isochoric	298	0.85	0.35	99.6	—
60	Isochoric	298	0.85	0.35	100	—
61	Isochoric	298	0.85	0.35	100	—
62	Isochoric	298	0.85	0.35	100	—
63	Isochoric	298	0.85	0.35	100	—
64	Isochoric	298	0.85	0.35	99.6	—
65	Isochoric	298	0.85	0.35	100	—
66	Isochoric	298	0.85	0.34	100	—
67	Isochoric	298	0.85	0.30	99.4	—
68	Isochoric	298	0.85	0.35	100	—
69	Isochoric	298	0.85	0.24	100	—
70	Isochoric	298	0.85	0.19	100	—
71	Isochoric	298	0.85	0.24	97.2	—
72	Isochoric	298	0.85	0.36	98.3	—
73	Isochoric	298	0.85	0.33	98.7	—
74	Isochoric	298	0.85	0.71	100	—
75	Isochoric	298	0.85	0.32	99	—

Table 3 (*continued*)

Entry	Method	T/K	p/bar	b_{gas}/mmol g^{-1}	β/%	ΔH_{abs}/kJ mol^{-1}
76	Isochoric	298	0.85	0.18	100	—
77	Isochoric	298	0.85	0.47	99.7	—
78	Isochoric	298	0.85	0.47	100	—
79	Isochoric	298	0.85	0.46	99.4	—
80	Isochoric	298	0.85	0.46	99.7	—
81	Isochoric	298	0.85	0.46	100	—
82	Isochoric	298	0.85	0.46	100	—
83	Isochoric	298	0.85	0.46	100	—
84	Isochoric	298	0.85	0.22	100	—
85	Isochoric	298	0.85	0.22	100	—
86	Isochoric	298	0.85	0.21	99	—
87	Isochoric	298	0.85	0.21	99	—
88	Isochoric	298	0.85	0.21	99	—
89	Isochoric	298	0.85	0.21	99	—
90	Isochoric	298	0.85	0.22	100	—
91	Isochoric	298	0.85	0.31	100	—
92	Isochoric	298	0.85	0.31	100	—
93	Isochoric	298	0.85	0.30	99.4	—
94	Isochoric	298	0.85	0.31	100	—
95	Isochoric	298	0.85	0.31	100	—
96	Isochoric	298	0.85	0.32	100	—
97	Isochoric	298	0.85	0.31	100	—
98	Isochoric	298	0.85	0.23	100	—
99	Isochoric	298	0.85	0.20	100	—
100	Isochoric	298	0.85	0.21	100	—
101	Isochoric	298	0.85	0.19	99.8	—
102	Isochoric	298	0.85	0.21	100	—
103	Isochoric	298	0.85	0.19	100	—
104	Isochoric	298	0.85	0.21	100	—
105	Isochoric	298	0.85	0.73	100	—
106	BET Micromeritics	273	20[c]	5.0	100	—
107	BET	nr	0.92	0.13[d]	95	—
118	Gravimetric (IGA)	298	10	1.06	96	—
119	Gravimetric (IGA)	303	5	0.35, 0.43	76, 72	−14.0, −14.4
120/125	Gravimetric (IGA)	303	5	0.39	75	−9.3
121	Gravimetric (IGA)	303	5	0.32	75	—
122	Gravimetric (IGA)	303	2	1.51	100	—
124	Gravimetric (IGA)	303	5	0.35	80	−9.9
126	Gravimetric (IGA)	303	5	0.32	80	−11.6
127	Breakthrough	298	1	5.8, 7.1, 8.8, 9.5	—	—
129	BET Quantachrome	298–303	1	0.19	—	—
130	BET Quantachrome	298–303	1	0.16	—	—
131	BET Quantachrome	298–303	1	0.16	—	—
132	BET Quantachrome	298–303	1	0.14	—	—
133	BET Quantachrome	298–303	1	0.20, 0.28	51, 54	—
134	BET Quantachrome	298–303	1	0.20	51	—
135	BET Quantachrome	298–303	1	0.18	54	—
136	BET Quantachrome	298–303	1	0.08	7	—
137	BET Quantachrome	298–303	1	0.07	26	—
138	BET Quantachrome	298–303	1	0.07	10	—
139	BET Quantachrome	298–303	1	0.08	41	—
140	BET Quantachrome	298–303	1	0.07	42	—
141	BET Quantachrome	298–303	1	0.09	7	—
142	BET Quantachrome	298–303	1	0.08	2	—
143	BET Quantachrome	298–303	1	0.11, 0.17	40, 41	—
144	BET Quantachrome	298–303	1	0.17, 0.21	42, 37	—
145	BET Quantachrome	298–303	1	0.11	44	—
146	BET Quantachrome	298–303	1	0.10	21	—
147	BET Quantachrome	298–303	1	0.20	51	—
148	BET Quantachrome	298–303	1	0.07	—	—
149	BET Quantachrome	298–303	1	0.21	—	—
150/151	Breakthrough	298	10	0.42[b], 1.48[b], 2.46[b]	—	—
152	Gravimetric (IGA)	303	5	0.47	100	—

In the table, nr = non reported. [a] Estimated using the density of glycol because the density of the suspension was not reported. [b] Calculated using the the second Virial coefficient[30] at the given temperature and absorption in cm^3 g^{-1}. [c] Relative pressure (P/P^0). [d] Mesitylene/ZIF-67-IDip(6%).

found adsorbed in cavities and on the surface of the suspended MOF and could easily be removed of the suspension by increasing the temperature to just 200 °C, whereas in the pure solid higher temperatures are needed to recover the adsorbed I_2.

Suspensions of ZIF-8 in glycol and glycol-mIm have proven to efficiently remove CO_2 from gas mixtures at pressures up to 50 bar at 298 K, showing excellent selectivities for several gas pairs, *e.g.* CO_2/H_2 = 951, CO_2/N_2 = 394 and CO_2/CH_4 = 114. These results can only be explained by favourable interactions of CO_2 with ZIF-8, the liquid solvents or both, the enhanced CO_2 absorption being associated to the free volume of the porous liquid material.[5,14]

Remarkable increases in CO_2 absorption, when compared to those of the pure solvents, are also found when using other liquids to suspend chosen porous solids. Because this enhancement is due to the free volume of the solid scaffold, the gas absorption is in general not selective unless specific interactions exist between the gas and the porous solid in the suspension. Knebel *et al.*[13] have used other properties of the 6%w/w ZIF-67-IDip suspension in mesitylene to separate gaseous mixtures. When using a dynamic breakthrough experiment to separate mixtures of methane, CH_4, and propylene, C_3H_6, they measured longer retention times for C_3H_6 in the suspensions (8.4 min longer than CH_4 in the conditions reported) than in pure mesitylene (just 2.5 min longer than CH_4). The difference in the breakthrough times has been attributed to the presence of permanenent porosity in the liquid since methane and propylene are only sparsely soluble in mesitylene and allows the separation of the two gases using this dynamic technique.[13] Porous liquids formed by 12.5%w/w of Al(fum)(OH) or by 12.5%w/w of HKUST-1 in PDMS also showed potential for CO_2 separation from natural gas with a relatively easy regeneration of the absorbent. The suspensions presented $\geq$75% recovery in CO_2 absorption capacities only after 2 h vacuum, whereas the conventional amine-based solution (12.5%w/wMEAin H_2O) only shows an $\approx$5% recovery. Cahir *et al.*[10] report that the suspension of 12.5%w/w Al(fum)(OH) in PDMS shows enhanced performance in both CO_2 absorption and selectivity, compared to the benchmark liquid material used for natural gas sweetening, Genosorb 1753 (dimethylether polyethylene glycol), at 348 to 298 and 5 to 1, respectively. He *et al.*[4] report that the suspensions of the decorated MOF UiO-66(185)@xPDMS in the liquid polymer PDMS4k, exhibits 13 and 8 times increase in CO_2 and Xe absorption when compared to the pure polymer at 273 K and 1 bar.

The porosity of the suspensions can be increased by increasing the solid concentration, which leads to an enhancement of the gas absorption capacity as shown by Shan *et al.*[15] who, by augmenting the concentration of ZIF-8 from 3.2 to 30%w/w in an ionic liquid, improved CO_2 absorption from 0.49 to 1.56 mmol g^{-1} at 10 and 298 K. This observation confirms that pores exist in the liquid phase and are correctly probed by the gas. Costa Gomes *et al.*[12] reported an enhancement from 0.37 to 0.47 mmol g^{-1} of CO_2 for suspensions containing 2 and 5%w/w ZIF-8 in $[P_{6,6,6,14}][NTf_2]$ at 5 bar and 303 K, respectively. Avila *et al.*[8] confirmed these observations for CO_2 and measured an increase of CH_4 absorption from 0.13 to 0.17 mmol g^{-1} at 5 bar and 303 K by increasing ZIF-8 concentration from 5 to 10%w/w in $[P_{6,6,6,14}][NTf_2]$.

Interestingly enough, the free volume of the porous solid dispersed is often not fully available in the porous suspension as indicated in Table 3 by the parameter β calculated as:[8]

$$\beta = \frac{n_{gas}^{MOF}/w_{MOF}}{b_{gas}^{pureMOF}} \quad (1)$$

where w_{MOF} is the weight fraction of MOF in the porous liquid. Shan *et al.*[15] showed that suspensions of ZIF-8 in [DBU-PEG][NTf_2] are not able to absorb the expected CO_2 absorption capacity, which is calculated considering the gas absorption in the pure ionic liquid and the in pure MOF are maintained. If we consider that the ionic liquid keeps its full capacity in the suspension, the differences between experimental and expected gas absorption in the suspensions correspond to the MOF absorbing 96% (in the 3.2%w/w suspension), 88% (in the 10%w/w suspension), 75% (in the 20%w/w suspension) and 70% (in the 30%w/w suspension) of its full capacity at 10 bar and 298 K. Similar results were found, both for CO_2 and CH_4, by Avila *et al.*[8] and Zhou *et al.*[7] for suspensions of 5%w/w ZIF-8 in $[P_{6,6,6,14}][NTf_2]$, $[P_{6,6,6,14}][Cl]$, $[P_{6,6,6,14}][Br]$ and $[P_{4,4,4,8}][NTf_2]$ and of 5%w/w HKUST-1 in $[P_{6,6,6,14}][NTf_2]$, with gas absorptions corresponding only to about 70–80% of the MOF's full capacity. The increase in the ZIF-8 concentration from 5%w/w to 10%w/w lead to an average ZIF-8 capacity in the pressure range 0.5 to 5 and at 303 K of 73 to 68% for CO_2 and 80 to 75% for CH_4 in suspensions of ZIF-8 in $[P_{6,6,6,14}][NTf_2]$, respectively (see Table 2). Cahir *et al.*[10] reported several porous suspensions for which CO_2 absorption corresponds to 100% of the solid being available and similar observations were reported by Avila *et al.*[6] for stable porous suspensions of ZIF-8 in $[P_{4,4,4,4}][Lev]$, an ionic liquid containing a symmetric, relatively small phosphonium cation capable of chemically reacting with CO_2.

The partial availability of the solid pores in the suspension can be attributed to the liquid partially blocking the pores or to the growing of the suspended solid aggregates to obstruct some of the pore apertures. This last hypothesis is not valid for stable suspensions of ZIF-8 in $[P_{6,6,6,14}][NTf_2]$ or in $[P_{4,4,4,4}][Lev]$ that remain stable for several months with aggregates of constant size.[6,8] In order to understand why the solid is not fully available for gases in the suspensions, we present in Fig. 4 details of molecular dynamics simulations of both $[P_{6,6,6,14}][NTf_2]$ (left) and $[P_{4,4,4,4}][NTf_2]$ (right) near a slab of ZIF-8. Different structures can be identified when $[P_{6,6,6,14}]+$ or $[P_{4,4,4,8}]+$ cations are present. In the first case, the apertures of ZIF-8 exposed to the liquid are filled with the non-polar, voluminous domains of the ionic liquid while in $[P_{4,4,4,4}][NTf_2]$ both the cation and the anion stay near solid entry pores. The consequence, as far as gas absorption by the porous suspension is concerned, is related with the nature of the gas. CO_2 is preferably solvated in the polar domains of the ionic liquids,[8,31] and so approaching the suspended solid's apertures is more difficult in $[P_{6,6,6,14}][NTf_2]$ than in $[P_{4,4,4,4}][NTf_2]$.

CO_2 absorption in porous liquids formed by zeolites ZSM-5 and Silicate-1 in [DBU-PEG][NTf_2] is also the expected considering

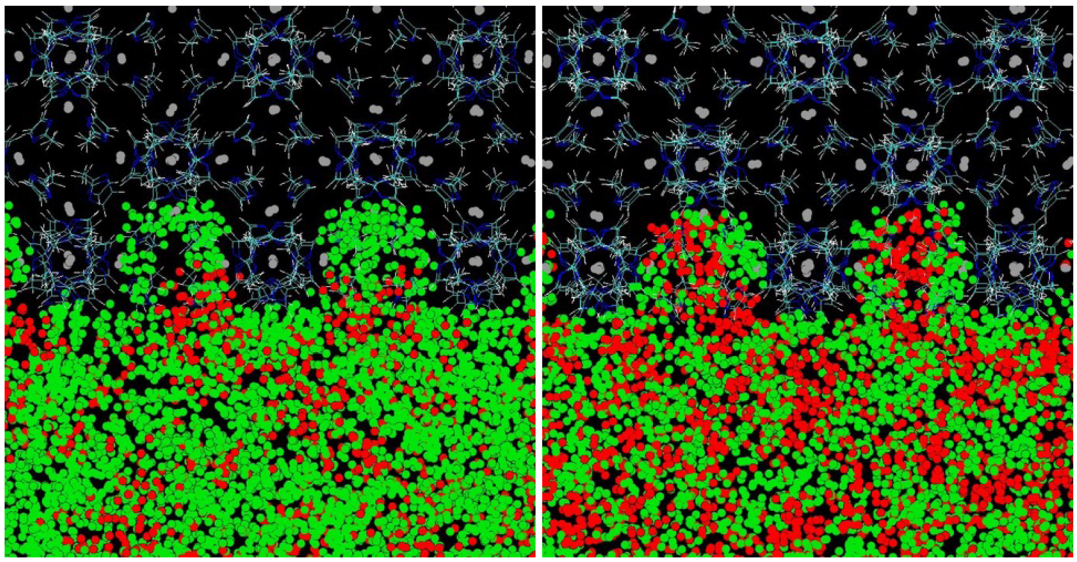

Fig. 4 Details of snapshots of $[P_{6,6,6,14}][NTf_2]$ (left) and $[P_{4,4,4,4}][NTf_2]$ (right) near a slab of ZIF-8. The polar (red) and apolar (green) domains of the ionic liquids are also depicted in the snapshots.

a full capacity of the solids in the suspensions.[15] Differently from the zeolitic imidazole-framework ZIF-8, the structures of zeolites ZSM-5 and Silicate-1 are characterized by a three-dimensional network of channel/cavities of 4.5 to 6—ZSM-5 has straight 10-ring 5.2 × 5.7 Å channels connected by sinusoidal 5.3 × 5.6 Å channels with intersection cavities of *ca.* 9 Å. Thus, the fully availability of the zeolites pores in suspension with the IL in comparison with ZIF-8 must be due to the structure of the superficial pores, as it was the case of different anchoring process of assymetric branched phosphonium ionic liquids.

He *et al.*[4] observed that polymer coated zirconium-based MOFs dispersed in PDMS4k did not present the entire MOF capacity for absorbing CO_2, instead showing 82.9%, 78.9% or 85.2% of the expected capacities, depending on the solid's concentrations. The discrepancy between the expected gas absorptions and the experimental values was attributed to the partial infiltration of of PDMS–shell to the surface layers of MOF pores which restricts the diffusion of the gas through the interface.

Different authors report viscosity increases with increasing solid concentration in MOF–polymer suspensions. He *et al.*[4] found increases from 0.05 Pa s (pure solvent) to *ca.* 7 Pa s (porous liquid) containing 33%w/w of the porous material and to *ca.* 30 Pa s (porous liquid) containing 50%w/w at 298 K. In a suspension of 40%w/w H-SZM-5-liquid in $[P_{6,6,6,14}][Br]$, the viscosity reaches 9.55 Pa s against 2.8 Pa s of the pure ionic liquid at 298 K. A considerably reduction to 0.81 been observed at 363 K.[20] Suspensions of 1 to 6%w/w of ZIF-67-IDip in Mesitylene also show an increase in viscosity from 0.16 Pa s to about 22 Pa s at low shear rates and from 0.004 Pa s to 0.011 Pa s at high shear rates.[13] Viscosity explains marked hysteresis in CO_2 absorption and desorption isotherms in suspensions of ZIF-8, ZSM-5 and Silicate-1 in $[DBU\text{-}PEG][NTf_2]$.[15]

Carbon dioxide absorption can be dramatically improved by preparing porous ionic liquids using salts that can chemically react with the gas. This is the case of phosphonium carboxylate ionic liquids that can reversibly chemisorb CO_2 while stabilizing solid MOFs, resulting in porous liquids behaving as high-performance absorbers.[6] Carboxylate anions combined with imidazolium cations are long known to be sufficiently basic to abstract the acidic proton from the cation in the presence of CO_2, promoting a chemical reaction between the ionic liquid and the gas. In a 1 : 2 CO_2 : IL reaction mechanism a carboxylic acid and a zwiterionic species are formed due to the carboxylation of the cation by CO_2. A weak equilibrium constant of about 75 at 303 K for $[C_4C_1im][OAc]$ points towards an easily reversible chemissorption process.[32]

More recently, Yeadon *et al.*[33] and Avila *et al.*[6] showed that phosphonium carboxylate ionic liquids are also able to react with CO_2 following a similar reaction mechanism involving the abstraction of the phosphonium $\alpha(CH_2)$-proton with a sufficiently low equilibrium constant to allow the low energy regeneration of the absorbent material. Care must, nevertheless be taken in engineering the carboxylate-based ionic liquids to be used in reactive porous liquids as bulky reaction products are necessary to preserve the permanent porosity after chemisorption of a gas. Avila *et al.*[6] have shown that low molar volume reaction products can enter the internal cavities of the solid scaffolds and eradicate porosity in the suspension. In this case, CO_2 absorption is not enhanced in the suspension of ZIF-8 in $[P_{4,4,4,4}][OAc]$ because the gas reacts with the ionic liquid to form acetic acid that enters the pores of ZIF-8. When replacing the $[OAc]^-$ by the voluminous $[Lev]^-$ anion where 5%w/w of ZIF-8 was suspended, high CO_2 absorption at low-pressures was observed with values comparable to those of alkanolamines at 2 bar and 303 K. The porous ionic liquid was easily regenerated under vacuum. Most of the carbon dioxide absorbed by the porous ionic liquid reacts with the carboxylate-based ionic liquids, the enhancement corresponding to the free

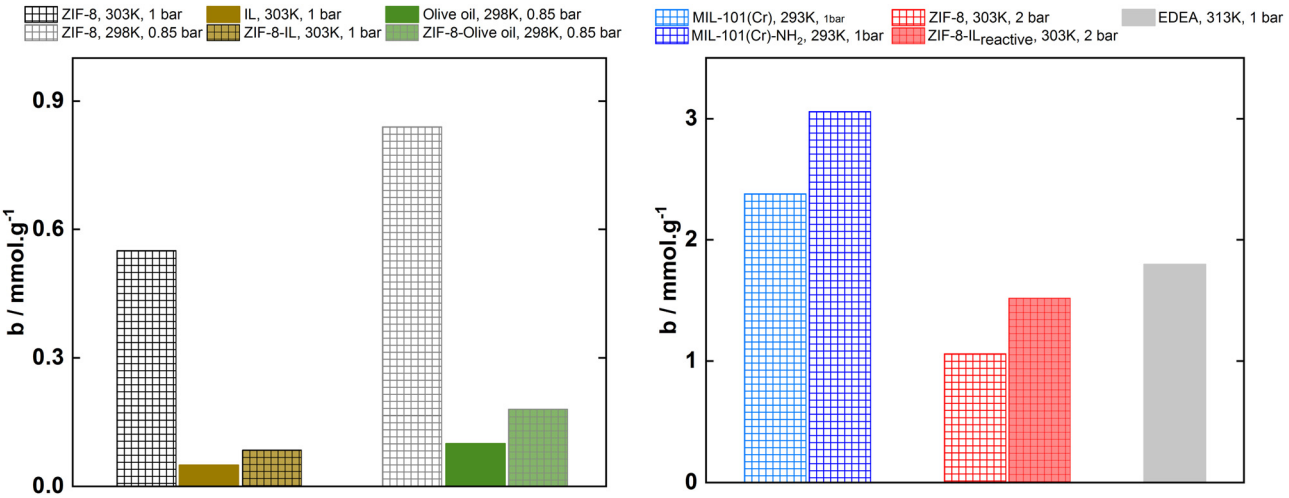

Fig. 5 (Left) Physically adsorbed–absorbed CO_2 by the pure MOF ZIF-8, the pure liquids IL:$[P_{6,6,6,14}][NTf_2]$[6] and olive oil[10] and by the porous liquids MOF + liquids containing 10%w/w and 12.5%w/w MOF concentration, respectively. (Right) Chemically adsorbed–absorbed CO_2 by a reactive MOF – MIL-101(Cr)-NH_2 surface functionalised with amine -NH_2 groups – compared to the pure MOF (MIL-101(Cr)),[34] a reactive porous liquid ZIF-8 + $IL_{reactive}$:$[P_{4,4,4,4}][Lev]$ compared to the pure ZIF-8[8] and by a 30 wt% *N*-ethyl-diethanolamine aqueous solution (EDEA),[28] a benchmark material used in CO_2 capture.

gas present in the pores of the liquid absorbent.[6] Fig. 5 illustrates the advantages of using functionalized MOFs and ionic liquids to chemisorb CO_2 and increase their capacities when compared with pure ionic liquids or porous liquids capable of only physically absorb the gas.

The possibility of having large CO_2 capacities in a porous liquid that both chemically and physically absorb the gas points towards new applications. Recently Zhou *et al.*[7] proposed a one-pot catalytic coupling of CO_2 and styrene epoxide to form styrene carbonate using porous ionic liquids. Mild reaction conditions and complete conversion/selectivity were achieved within 3 hours timeframe using only 5%w/w of ZIF-8 in $[P_{6,6,6,14}][Cl]$ at 80 °C and atmospheric pressure of CO_2 or 2%w/w of ZIF-8 at 80 °C and 10 bar of CO_2. The dramatic activity and selectivity enhancement over pure conventional ammonium halide catalysts (23% to 44% conversion and 24% to 42% selectivity) or over pure ionic liquids (100% conversion and 64–75% selectivity) can be explained by the presence of empty cavities in the liquid capable of acting as CO_2 reservoir concomitantly with the presence of Lewis acidic sites in the ZIF-8 structure that act as co-catalyst to activate the epoxide.

Through the assembly of zeolite nanosheets with $[N_{8,8,8,1}][Cl]$, Chen *et al.*[25] also performed catalytic reactions using type III porous liquids. A one pot cascade decetalization-Knoevenagel/Aldol condensation outperformed traditional systems, reaching >90% conversion of the belzaldehyde dimethylacetal and selectivity of the benzilidene malonitrile at 80 °C using only 30 mg of the porous liquid MCM-22-PL(26%w/w). The catalyst was easily recovered by evaporating the solvent and products by heating under vacuum, which lead to a 94% selectivity after been reused for five times. The high catalytic activity lying in the presence of acidic and basic sites, the abundant cavity distribution ensuring the rapid mass transfer and the combined properties of both homogeneous and heterogeneous catalysis.

Type III porous liquids have also been investigated for water/alcohol separations[17] and desulfurization of fuels.[26] By the use of ZIF-8 + $[Bpy][NTf_2]$ porous liquid, Wang *et al.*[17] achieved 88% of extraction of a valuable fluoride alcohol, 2,2,3,3-tetrafluoro-1-propanol, from wastewater. The fluoroalcohol–water azeotropic system was efficiently separated due to the unique liquid pore property and strong intermolecular interactions among the porous solid, the ionic liquid and the alcohol. Yang *et al.*[26] used ZIF-8 (surface modified by phophomolybdic acid, HPMo@ZIF-8) and $[Emim][NTf_2]$ to extract sulfides from a fuel oil. While the most widely used method of hydrodesulurization requires harsh reaction conditions, high hydrogen and energy consumption, the porous liquid removed 100% of dibenzothiophene sulfur from a model oil in only 2 h at ambient conditions. The excellent extraction performance is attributed to the dispersion of catalytically active centers, the fluidity of the material and the extraction ability of ionic liquids. In both water/alcohol and desulfurization applications, the porous liquid were easily recovered and reused several times.

All these findings support numerous potential applications of type III porous liquids in liquid-bed-based gas separation[16] with the possibility of easy and low *in situ* regeneration process for the porous liquids and definitely resolving one of the major drawbacks for amine-based CO_2 scrubbing technologies related to the large energy cost for regeneration.[5,6,10] Low environmental impact or even biocompatible porous liquid will most certainly open new possibilities for future applications of these composite materials.[10,11]

3 Conclusions

More than one hundred and fifty type III porous liquids based on suspensions of porous scaffolds in different liquids have

been prepared so far. The preparation of such porous suspensions is more or less straightforward depending on the materials and mainly consists on the dispersion, by ultrasound or mechanical stirring, of small solid particles in the liquid. In the large majority of the cases the authors report that the solid structure is maintained in the suspension, even when the suspensions are not stable during a significant amount of time.

The porosity of the liquid phases is generally probed by measuring the gas solubility in the pure liquid and comparing it with the absorption of the same gas by the suspension. In all the reported cases, the gas absorption is significantly higher than that of the pure liquid, the increase being proportional to the amount of solid dispersed. In some cases it was observed that a small percentage of the porous solid is not available to absorb the gas in the suspension, probably due to the accumulation of the liquid near the solid's pore apertures or by a partial aggregation of the particles in suspension. These phenomena are observed in different porous suspensions, independently of the solids and liquids used in their preparation.

The porous suspensions prepared using molecular solvents so far are seldom stable for more than one to two days. When prepared using ionic liquids, the porous liquid suspensions often remain stable for several months. It was possible, using precise microcalorimety measurements and molecular simulation to show that the mechanisms that explain this stability in porous suspensions of MOFs in ionic liquids are complex and linked not only with the solid–ionic liquid interactions but also with the structure of the liquid near the exposed solid surfaces. Different authors observed that ionic liquids can also stabilize suspensions of zeolites even if these solids are known for strongly aggregate ought to favorable particle–particle interactions.

Recent work combines chemistry and permanent porosity to enhance the capacity of porous ionic liquids to absorb gases such as carbon dioxide. The capacity of such porous suspensions that remain stable for more than twenty months is similar to that of benchmark aqueous solutions of alkanolamines at very low partial pressures of the gas. The porous ionic liquid absorbent being regenerated at room temperature through a mild pressure swing cycle. Porous ionic liquids have been also described as a powerful reaction media combining high gaseous capacities with good properties as organocatalysts. High activity and selectivity to capture and transform CO_2 under mild reaction conditions points towards a new promising, high-performing, sustainable family of absorbents.

Some authors claim that in composites formed by nanoporous solids and ionic liquids, the salt can impregnate the solid pores leading, in some cases, to an enhancement in the gas sorption that can not be easily explained. For example, Harmanli *et al.*[35] claim that the enhancement of gas absorption is such that it even surpasses the capacity of the pure solid. This surprising observation is just the result of normalizing the gas uptake by the mass of the ionic liquid, one of the two components of the composite. When correctly normalizing by the total mass of the composite and comparing it with the pure ionic liquid and the pure solid capacities of absorbing N_2, the composite absorb more gas than the pure liquid and less than the pure porous solid. Koyuturk *et al.*[36] also reported CO_2 uptake higher than the pure solid in [BMIM][BF_4]/ZIF-8 composites, which can be due to the small addition of the IL capacity of absorbing the gas. Although in both cases the amount of liquid is lower than that of the solid (differently from the porous liquid suspensions reported above), the authors report that the solid integrity is maintained in the composite and the gas absorption values are in line with that of the reported porous liquids with no need to claim imprecise synergistic effects. This observation shows that, probably, other type 3 porous liquids have been prepared but have not been reported as such by the authors.

We conclude that type III porous liquids are not just another family of porous materials but instead one that can be considered for many new applications including gas separations, reaction media for gaseous solutes or *in vivo* delivery of small molecules. Important work is ongoing in several research groups concerning the understanding of the design rules for porous suspensions for different applications.

Author contributions

R. C. and A. P. performed the molecular simulations, described the simulation work in the manuscript, and helped review the manuscript. J. A. performed the experimental measurements. J. A. and M. C. G. planned the experiments, reviewed the literature and wrote the manuscript.

Conflicts of interest

There are no conflicts to declare.

Acknowledgements

M. C. G. and J. A. thank IDEX-LYON for financial support (Programme Investissements dAvenir ANR-16-IDEX-0005). MD simulations were performed on the Pôle Scientifique de Modélisation Numérique (PSMN) at ENS de Lyon.

Notes and references

1 N. O'Reilly, N. Giri and S. L. James, *Chem. – Eur. J.*, 2007, **13**, 3020–3025.
2 N. Giri, M. G. Del Pópolo, G. Melaugh, R. L. Greenaway, K. Rätzke, T. Koschine, L. Pison, M. F. Gomes, A. I. Cooper and S. L. James, *Nature*, 2015, **527**, 216–220.
3 A. I. Cooper, *ACS Cent. Sci.*, 2017, **3**, 544–553.
4 S. He, L. Chen, J. Cui, B. Yuan, H. Wang, F. Wang, Y. Yu, Y. Lee and T. Li, *J. Am. Chem. Soc.*, 2019, **141**, 19708–19714.
5 M. Z. Ahmad and A. Fuoco, *Curr. Res. Green Sustain. Chem.*, 2021, **4**, 100070.
6 J. Avila, L. F. Lepre, C. Santini, M. Tiano, S. Denis-Quanquin, K. Chung Szeto, A. Padua and M. Costa Gomes, *Angew. Chem., Int. Ed.*, 2021, 12876–12882.

7 Y. Zhou, J. Avila, N. Berthet, S. Legrand, C. C. Santini, M. Costa Gomes and V. Dufaud, *Chem. Commun.*, 2021, **57**, 7922–7925.
8 J. Avila, C. Červinka, P. Y. Dugas, A. A. Pádua and M. Costa Gomes, *Adv. Mater. Interfaces*, 2021, **8**, 1–15.
9 A. Bavykina, A. Cadiau and J. Gascon, *Coord. Chem. Rev.*, 2019, **386**, 85–95.
10 J. Cahir, M. Y. Tsang, B. Lai, D. Hughes, M. A. Alam, J. Jacquemin, D. Rooney and S. L. James, *Chem. Sci.*, 2020, **11**, 2077–2084.
11 K. Jie, Y. Zhou, H. P. Ryan, S. Dai and J. R. Nitschke, *Adv. Mater.*, 2021, **33**, 1–18.
12 M. Costa Gomes, L. Pison, C. Červinka and A. Padua, *Angew. Chem., Int. Ed.*, 2018, **57**, 11909–11912.
13 A. Knebel, A. Bavykina, S. J. Datta, L. Sundermann, L. Garzon-Tovar, Y. Lebedev, S. Durini, R. Ahmad, S. M. Kozlov, G. Shterk, M. Karunakaran, I. D. Carja, D. Simic, I. Weilert, M. Klüppel, U. Giese, L. Cavallo, M. Rueping, M. Eddaoudi, J. Caro and J. Gascon, *Nat. Mater.*, 2020, **19**, 1346–1353.
14 H. Liu, B. Liu, L. C. Lin, G. Chen, Y. Wu, J. Wang, X. Gao, Y. Lv, Y. Pan, X. Zhang, X. Zhang, L. Yang, C. Sun, B. Smit and W. Wang, *Nat. Commun.*, 2014, **5**, 1–7.
15 W. Shan, P. F. Fulvio, L. Kong, J. A. Schott, C. L. Do-Thanh, T. Tian, X. Hu, S. M. Mahurin, H. Xing and S. Dai, *ACS Appl. Mater. Interfaces*, 2018, **10**, 32–36.
16 S. Liu, J. Liu, X. Hou, T. Xu, J. Tong, J. Zhang, B. Ye and B. Liu, *Langmuir*, 2018, **34**, 3654–3660.
17 Z. Wang, P. Zhao, J. Wu, J. Gao, L. Zhang and D. Xu, *New J. Chem.*, 2021, **45**, 8557–8562.
18 X. Li, D. Wang, Z. He, F. Su, N. Zhang, Y. Xin, H. Wang, X. Tian, Y. Zheng, D. Yao and M. Li, *Chem. Eng. J.*, 2021, **417**, 129239.
19 R. E. Mow, A. S. Lipton, S. Shulda, E. A. Gaulding, T. Gennett and W. A. Braunecker, *J. Mater. Chem. A*, 2020, **8**, 23455–23462.
20 P. Li, H. Chen, J. A. Schott, B. Li, Y. Zheng, S. M. Mahurin, D. E. Jiang, G. Cui, X. Hu, Y. Wang, L. Li and S. Dai, *Nanoscale*, 2019, **11**, 1515–1519.
21 X. Li, D. Wang, H. Ning, Y. Xin, Z. He, F. Su, Y. Wang, J. Zhang, H. Wang, L. Qian, Y. Zheng, D. Yao and M. Li, *Sep. Purif. Technol.*, 2021, **276**, 119305.
22 B. Lai, J. Cahir, M. Y. Tsang, J. Jacquemin, D. Rooney, B. Murrer and S. L. James, *ACS Appl. Mater. Interfaces*, 2021, **13**, 932–936.
23 P. Li, D. Wang, L. Zhang, C. Liu, F. Wu, Y. Wang, Z. Wang, Z. Zhao, W. Wu, Y. Liang, Z. Li, W. Wang and Y. Zheng, *Small*, 2021, **17**, 1–5.
24 A. Kai, B. D. Egleston, A. Tarzia, R. Clowes, M. E. Briggs, K. E. Jelfs, A. I. Cooper and R. L. Greenaway, *Adv. Funct. Mater.*, 2021, **2106116**, 2106116.
25 H. Chen, Z. Yang, H. Peng, K. Jie, P. Li, S. Ding, W. Guo, X. Suo, J. Liu, R. Yan, W. Liu, C. L. Do-Thanh, H. Wang, Z. Wang, L. Han, W. Yang and S. Dai, *Chem*, 2021, **7**, 3340–3358.
26 N. Yang, L. Lu, L. Zhu, P. Wu, D. Tao, X. Li, J. Gong, L. Chen, Y. Chao and W. Zhu, *Inorg. Chem. Front.*, 2022, **9**, 165–178.
27 K. J. Fraser and D. R. MacFarlane, *Aust. J. Chem.*, 2009, **62**, 309–321.
28 B. Dutcher, M. Fan and A. G. Russell, *ACS Appl. Mater. Interfaces*, 2015, **7**, 2137–2148.
29 I. Kim, K. A. Hoff, E. T. Hessen, T. Haug-Warberg and H. F. Svendsen, *Chem. Eng. Sci.*, 2009, **64**, 2027–2038.
30 J. H. Dymond, K. N. Marsh, R. C. Wilhoit and K. C. Wong, *The Virial Coefficients of Pure Gases*, Springer, Berlin, 2002, vol. 21A, p. 380.
31 D. Almantariotis, T. Gefflaut, A. A. Pádua, J. Y. Coxam and M. F. Costa Gomes, *J. Phys. Chem. B*, 2010, **114**, 3608–3617.
32 L. F. Lepre, J. Szala-Bilnik, L. Pison, M. Traïkia, A. A. Pádua, R. A. Ando and M. F. Costa Gomes, *Phys. Chem. Chem. Phys.*, 2017, **19**, 12431–12440.
33 D. J. Yeadon, J. Jacquemin, N. V. Plechkova, M. Maréchal and K. R. Seddon, *ChemPhysChem*, 2020, **21**, 1369–1374.
34 A. Khutia and C. Janiak, *Dalton Trans.*, 2014, **43**, 1338–1347.
35 I. Harmanli, N. V. Tarakina, M. Antonietti and M. Oschatz, *J. Am. Chem. Soc.*, 2021, **143**, 9377–9384.
36 B. Koyuturk, C. Altintas, F. P. Kinik, S. Keskin and A. Uzun, *J. Phys. Chem. C*, 2017, **121**, 10370–10381.